

This is a repository copy of *Water-Soluble Organic Composition of the Arctic Sea Surface Microlayer and Association with Ice Nucleation Ability*.

White Rose Research Online URL for this paper:  
<http://eprints.whiterose.ac.uk/127892/>

Version: Accepted Version

---

**Article:**

Chance, Rosemary Jane [orcid.org/0000-0002-5906-176X](https://orcid.org/0000-0002-5906-176X), Hamilton, Jacqueline Fiona [orcid.org/0000-0003-0975-4311](https://orcid.org/0000-0003-0975-4311), Carpenter, Lucy Jane [orcid.org/0000-0002-6257-3950](https://orcid.org/0000-0002-6257-3950) et al. (3 more authors) (2018) *Water-Soluble Organic Composition of the Arctic Sea Surface Microlayer and Association with Ice Nucleation Ability*. *Environmental Science & Technology*. pp. 1817-1826. ISSN 1064-3389

<https://doi.org/10.1021/acs.est.7b04072>

---

**Reuse**

Items deposited in White Rose Research Online are protected by copyright, with all rights reserved unless indicated otherwise. They may be downloaded and/or printed for private study, or other acts as permitted by national copyright laws. The publisher or other rights holders may allow further reproduction and re-use of the full text version. This is indicated by the licence information on the White Rose Research Online record for the item.

**Takedown**

If you consider content in White Rose Research Online to be in breach of UK law, please notify us by emailing [eprints@whiterose.ac.uk](mailto:eprints@whiterose.ac.uk) including the URL of the record and the reason for the withdrawal request.

1 Water-soluble organic composition of the  
2 Arctic sea surface microlayer and association  
3 with ice nucleation ability

4

5 *Rosie J. Chance*<sup>\*1</sup>, *Jacqueline F. Hamilton*<sup>1</sup>, *Lucy J. Carpenter*<sup>1</sup>, *Sina C.*

6 *Hackenberg*<sup>1</sup>, *Stephen J. Andrews*<sup>1</sup>, *Theodore W. Wilson*<sup>2†</sup>

7

8 1. Wolfson Atmospheric Chemistry Laboratories, Department of Chemistry,

9 University of York, Heslington, York, YO10 5DD, UK.

10 2. School of Earth and Environment, University of Leeds, Woodhouse Lane, Leeds,

11 LS2 9TJ, UK.

12

13 †Now at Owlstone Medical Ltd., 162 Cambridge Science Park, Milton Road

14 Cambridge, CB4 0GH, UK.

15

16

17 \* Corresponding author: [rosie.chance@york.ac.uk](mailto:rosie.chance@york.ac.uk)

18

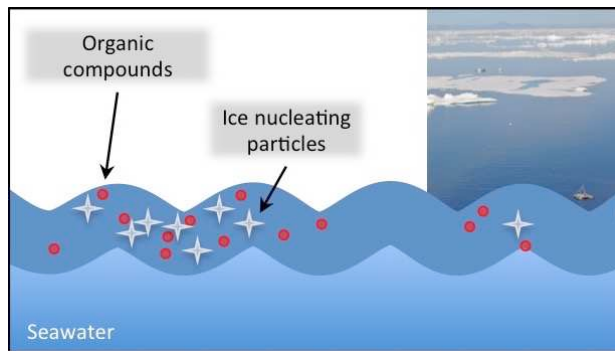
19 **Abstract**

20 Organic matter in the sea surface microlayer (SML) may be transferred to the  
21 atmosphere as sea spray and hence influence the composition and properties of  
22 marine aerosol. Recent work has demonstrated that the SML contains material  
23 capable of heterogeneously nucleating ice, but the nature of this material remains  
24 largely unknown. Water-soluble organic matter was extracted from SML and  
25 underlying seawater from the Arctic and analyzed using a combination of mass  
26 spectrometric approaches. High performance liquid chromatography-ion trap mass  
27 spectrometry (LC-IT-MS), and Fourier transform ion cyclotron resonance MS (FT-  
28 ICR-MS), showed seawater extracts to be compositionally similar across all stations,  
29 while microlayer extracts had a different and more variable composition. LC-IT-MS  
30 demonstrated the enrichment of particular ions in the microlayer. Ice nucleation  
31 ability (defined as the median droplet freezing temperature) appeared to be related to  
32 the relative abundances of some ions, although the extracts themselves did not retain  
33 this property. Molecular formulae were assigned using LC - quadrupole time-of-flight  
34 MS (LC-TOF-MS<sup>2</sup>) and FT-ICR-MS. The ice nucleation tracer ions were associated  
35 with elevated biogenic trace gases, and were also observed in atmospheric aerosol  
36 collected during the summer, but not early spring suggesting a biogenic source of ice  
37 nuclei in the Arctic microlayer.

38

39

40 **TOC/Abstract art**



41

## 42 **Introduction**

43 The sea surface microlayer (SML) is a thin layer of water at the sea-air interface in  
44 which chemical, physical and biological properties differ from those of the underlying  
45 seawater<sup>1</sup>. The SML has an operationally defined thickness of ~1 to ~1000  $\mu\text{m}$ <sup>1</sup>, and  
46 surfactant enrichments have been found to persist up to wind speeds of up to at least ~  
47  $13 \text{ m s}^{-1}$ <sup>2,3</sup>. It has been recognized as a distinct compartment for photochemical  
48 reactions<sup>4,5</sup> and biogeochemical transformations<sup>1</sup>.

49

50 As the SML lies at the interface between the ocean and the atmosphere, it is expected  
51 to influence the transfer of gases and particles between these compartments<sup>6-10</sup>.  
52 Material from the SML may become entrained in sea spray aerosol (SSA) generated  
53 by bubble bursting processes<sup>11</sup>, but the extent of the SML's direct contribution to SSA  
54 remains unknown<sup>12</sup>. In the central Arctic, atmospheric particles have been found to  
55 have similar properties to particles (~100 nm diameter) in the SML beneath,  
56 suggesting that the SML may be a significant source of these aerosol particles<sup>13</sup>.  
57 Similarly, co-variation of anionic surfactants in aerosol and the SML in the  
58 Mediterranean suggests the SML is a source of aerosol organic matter<sup>14</sup>.  
59 Photochemical and heterogeneous reactions in the microlayer may also supply  
60 volatile organic compounds (VOCs) to the atmosphere, and so contribute to  
61 secondary organic aerosol formation<sup>4,15,16</sup>.

62

63 The influence of the SML on air-sea exchange and marine aerosol properties is  
64 assumed to be a function of its chemical composition, but as yet, the composition of  
65 the microlayer has not been fully characterized. Relative to the underlying bulk  
66 seawater, the SML has been found to be enriched in a wide range of organic and

67 inorganic compounds (<sup>12</sup> and references therein; <sup>6, 17-27</sup>). Rising bubbles collect surface-  
68 active organic material from the water column and transfer it to the microlayer<sup>1, 2</sup>,  
69 where further enrichment and/or modification (e.g. by photochemical oxidation<sup>5</sup>, or  
70 microbial degradation<sup>1, 28</sup>) of some compound classes may occur. Non-targeted high-  
71 resolution mass spectrometry has shown a shift towards lower molecular weight  
72 compounds in the SML relative to the underlying seawater, thought to be the result of  
73 increased degradation<sup>22</sup>.

74

75 The microlayer is also enriched in biogenic material that can heterogeneously  
76 nucleate ice<sup>29</sup>. The presence of ice nucleating particles (INPs) in bulk seawater and  
77 marine air masses has long been known<sup>30-35</sup>, and recent studies indicate that the oceans  
78 are probably an important source of aerosolized atmospheric INPs, particularly in  
79 remote regions away from terrestrial sources<sup>29, 36-38</sup>. Depending on the exact nucleation  
80 pathway, heterogeneous ice nucleation by INPs can raise the temperature and/or  
81 lower the relative humidity at which ice crystals form in clouds, with consequent  
82 impacts on cloud lifetime, precipitation and cloud radiative properties. The identity of  
83 INPs in the SML, and the factors governing their abundance, remain unknown.

84

85 In this work, low mass resolution liquid chromatography mass spectrometry was used  
86 to explore the molecular composition of dissolved organic matter (DOM) isolated  
87 from Arctic SML and underlying seawater, with the aim of identifying features which  
88 related to ice nucleation activity, an atmospherically relevant property. A combination  
89 of high-mass resolution mass spectrometric techniques was then used to examine  
90 these features further. The work was conducted as part of the Aerosol-Cloud Coupling  
91 and Climate Interactions in the Arctic (ACCACIA) project.

92 **Experimental section**

93

94 **Sample collection**

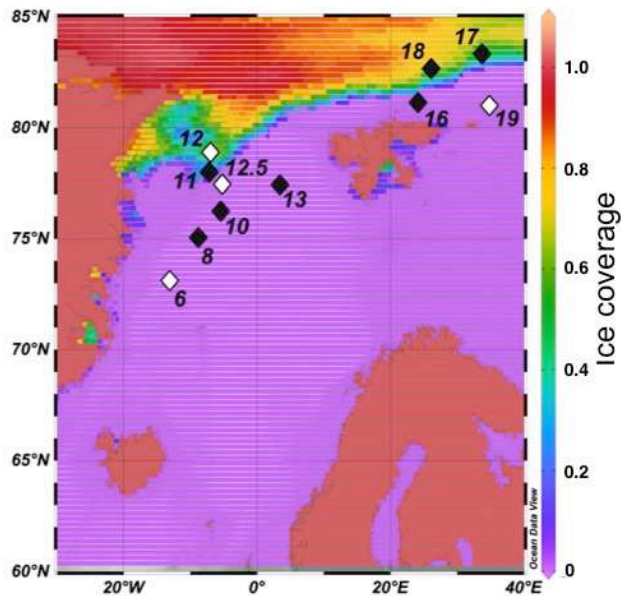
95 Samples were collected from the Greenland and Barents Seas during cruise JR288 of  
96 the RRS *James Clark Ross* in July-August 2013. Water sampling locations are shown  
97 in Figure 1 and further details are given in Table S1 of Supplementary Information  
98 (SI). Sea surface microlayer samples were collected using a remote controlled rotating  
99 drum type sampler deployed for approximately 40 minutes per sample<sup>29, 39</sup>. Sub-  
100 samples of ~1 L were taken for mass spectrometric analysis. Two sampling blanks  
101 ('boat blanks') were collected by running underlying seawater from the same location  
102 over the sampler drum, and consequently through the sampler's whole collection  
103 system. Underlying seawater was collected from approximately 2-5 m depth using  
104 Niskin bottles deployed on a CTD rosette. Seawater subsamples (~10 L) were  
105 collected from the Niskin bottles into dedicated clean glass sampling bottles that were  
106 rinsed with dilute HCl (10% v/v) prior to the start of the cruise.

107

108 Atmospheric aerosol samples were collected during cruise JR288, and also during a  
109 cruise to the same area made by the RV *Lance* in March 2013. Aerosol samples were  
110 collected onto pre-combusted quartz (Whatman QM-A) filters using a high volume  
111 aerosol collector (Ecotech Hi-vol 3000; air flow ~68 m<sup>3</sup> hr<sup>-1</sup>) fitted with a PM<sub>2.5</sub> size  
112 selective inlet. The sampler was located on the bridge-top deck of each ship, and  
113 automatically controlled according to wind direction in order to avoid contamination  
114 from the ship's stack. Individual samples were collected over 24 hour periods, with an  
115 average total air volume of 1261 m<sup>3</sup> per sample.

116

117  
118



119

120 **Figure 1.** Locations of sea surface microlayer sampling stations during cruise JR288,  
121 superimposed on NSIDC satellite sea ice concentration data for 28 July 2013. Sea ice  
122 concentrations are shown as fractional coverage, where 0 is no ice and 1 is complete  
123 cover; values >1 are masks for land and missing data. White station symbols indicate  
124 locations where the microlayer had particularly high relative ice nucleation activity,  
125 based on median freezing temperatures,  $T_{50}$ . Figure produced using Ocean data View  
126 <sup>40</sup>.

127

128

129

### 130 **Sample preparation**

131

132

133

134

135

Immediately following collection, all seawater and microlayer samples were filtered under vacuum through pre-combusted (5 hours at 450°C) Whatman GF/F filters (nominal pore size 0.7  $\mu\text{m}$ ). Dedicated acid washed glass bottles and a polycarbonate filter holder were used; all were acid rinsed at least every few days. Dissolved organic matter was isolated from the filtrate by solid phase extraction (SPE) onto Agilent



136 Bond Elut PPL cartridges, using LC-MS grade solvents (Fisher Optima), according to  
137 the method of Dittmar et al<sup>41</sup>. Procedural blanks were prepared by replacing the  
138 sample with ~5 mL of rinse solution (0.01M hydrochloric acid). The operationally  
139 defined fraction of the DOM isolated by this procedure is referred to as SPE-DOM.  
140 SPE extraction efficiency was not evaluated here, but a previous comparison of  
141 sorbents found the protocol adopted here to be the most efficient at extracting DOM  
142 from seawater, with average recoveries of 43 and 62% for coastal and open ocean  
143 waters respectively<sup>41</sup>. Longnecker et al<sup>42</sup> achieved DOM recoveries from Arctic  
144 seawater of 32 to 43% using a variation of this method with two SPE extraction steps.

145

146 Methanolic extracts were stored in pre-combusted glass vials at -20 °C for return to  
147 the UK. Prior to analysis, samples were evaporated to dryness using a vacuum solvent  
148 evaporator (Biotage, Sweden) and redissolved in methanol-water (1:1 mixture).  
149 Potential exists for organic matter to undergo molecular transformations, such as  
150 trans-esterification of carboxylic acids and esters<sup>43</sup>, and acetal and hemi-acetal  
151 formation<sup>44</sup>, in methanolic extracts. Some of these changes may occur very rapidly,  
152 over timescales of minutes, and so be effectively unavoidable. During longer-term  
153 storage, it has been shown that methanolic extracts may undergo proton exchange but  
154 not esterification or hemiacetal formation<sup>45</sup>. Repeat analyses of our samples after  
155 more than 12 months also suggests they are stable at -20 °C.

156

157 Aerosol samples were foil wrapped and frozen at -20°C immediately following  
158 collection for return to the UK. Aerosol material was extracted from the filters into  
159 ultrapure water (Fisher LC-MS grade) by ultrasonication, and then extracted by SPE  
160 as above. To allow direct comparison of seawater and aerosol SPE-DOM, the salinity

161 of the aqueous aerosol extracts was made up to that of seawater ( $\sim 35 \text{ g L}^{-1}$ ) by adding  
162 sodium chloride prior to SPE. As aerosol loadings were very low, extracts from three  
163 or four consecutive aerosol samples of the same air mass origin (assigned using air  
164 mass back trajectories from NOAA Hysplit <sup>46</sup>) were combined.

165

#### 166 **Mass spectrometric analysis**

167

168 *High performance liquid chromatography-ion trap mass spectrometry (LC-IT-MS).*

169 The SPE-DOM sample extracts were first analyzed by LC-IT-MS using an HCT Plus  
170 ion trap mass spectrometer (Bruker Daltonics GmbH, Bremen, Germany) coupled to  
171 an Agilent 1100 series HPLC. A Pinnacle DB-C<sub>18</sub> column with 5  $\mu\text{m}$  particle size  
172 (Restek, 4.6 x 150 mm) was used with 0.1% (v/v) formic acid in ultrapure water  
173 (Optima LC-MS grade, Fisher, UK) and methanol (Optima LC-MS grade, Fisher,  
174 UK) mobile phases and a flow rate of 0.6 mL min<sup>-1</sup>. Gradient elution was performed  
175 as follows: 0-13 minutes 20% methanol; 13-23 minutes increase to 60% methanol;  
176 23-33 minutes, hold at 60% methanol; 33-43 minutes increase to 100% methanol; 43-  
177 50 minutes hold at 100% methanol; 50-53 minutes return to starting conditions; 53-59  
178 minutes hold at starting conditions. Electrospray ionization was used with a source  
179 temperature of 365°C, nebulizer pressure of 70 psi and drying gas (N<sub>2</sub>) flow rate of 12  
180 L min<sup>-1</sup>. The mass spectrometer was operated in alternating positive and negative ion  
181 mode, with a scan range of  $m/z$  50 - 1000 and a target mass setting of  $m/z$  150. Mass  
182 calibration was conducted using a standard containing arginine clusters (Sigma-  
183 Aldrich). The mass accuracy ranged from  $\sim 100$  to 2000 ppm, and the mass resolution  
184 was 500 at  $m/z$  200.

185

186 *Fourier transform ion cyclotron resonance mass spectrometry (FT-ICR-MS)*. SPE-  
187 DOM extracts were also analyzed by ultra-high mass resolution FT-ICR-MS with  
188 electrospray ionization using a SolariX XR 9.4T instrument (Bruker Daltonics,  
189 Coventry, UK). Samples were introduced by direct infusion at a flow rate of  
190 120  $\mu\text{l hr}^{-1}$ . The source temperature was 220 °C, the nebulizer gas ( $\text{N}_2$ ) pressure was  
191 1.2 bar and the drying gas flow rate was 4 L  $\text{min}^{-1}$ . Samples were analyzed separately  
192 in positive and negative mode over a scan range of  $m/z$  58 to 1200. Each sample was  
193 analyzed twice, typically with 50 (negative mode) or 200 (positive mode) scans  
194 collected per analysis. The mass resolution was  $\sim 140,000$  at  $m/z$  200. The instrument  
195 was externally calibrated using sodium formate clusters. Negative mode FT-ICR-MS  
196 spectra were internally recalibrated using the ubiquitous series of DOM anions  
197 ( $\text{C}_{17}\text{H}_{19}\text{O}_8^-$ ,  $\text{C}_{18}\text{H}_{21}\text{O}_8^-$ ,  $\text{C}_{19}\text{H}_{23}\text{O}_8^-$  etc) proposed by Kujawinski et al., 2009<sup>47</sup>. Positive  
198 mode FT-ICR-MS spectra were internally calibrated using a combination of DOM  
199 and common contaminant ions (e.g. proline, arginine, polyethylene glycol oligomers).  
200 Aerosol SPE extracts were screened for selected ions using FT-ICR-MS in negative  
201 mode, with conditions as above. Due to a lack of suitable ions, internal mass  
202 calibration was not carried out for these samples.

203

204 Bulk compositional analysis was conducted for FT-ICR-MS data collected in the  
205 negative mode, as this has been more widely reported in comparable previous studies.  
206 Only  $m/z$  values that satisfied the following criteria were considered: (i) absent from  
207 the procedural extraction blank (at a signal to noise ratio of at least four); (ii) present  
208 in both analytical replicates; (iii) signal-to-noise ratio greater than ten. Molecular  
209 formulae were generated using the SmartFormula functionality within DataAnalysis  
210 4.1 software (Bruker Daltonics, Bremen, Germany), In addition to C, H and O, the

211 heteroatoms N, S and P were allowed, with a formula error limit of 1 ppm. Elemental  
212 combinations were restricted according to rules adopted from similar previous work<sup>22</sup>.  
213<sup>48-54</sup>, see SI for further details.

214

215 *High-performance liquid chromatography - quadrupole time-of-flight mass*  
216 *spectrometry (LC-TOF-MS<sup>2</sup>)*. A subset of microlayer and seawater extracts were  
217 analyzed by LC-TOF-MS<sup>2</sup> using a maXis 3G mass spectrometer (Bruker Daltonics,  
218 Coventry, UK) coupled to a Dionex ultimate 3000 HPLC system (Thermo Scientific  
219 Inc., UK). The column, mobile phases and gradient program were the same as those  
220 used for LC-IT-MS analysis (see above), with the exception that HPLC grade water  
221 (Fisher, UK) was used instead of LC-MS grade water. Differences in instrument  
222 plumbing resulted in a slight retardation of retention times of ~2 minutes.  
223 Electrospray ionization was used with a source temperature of 350°C, nebulizer  
224 pressure of 4 bar and drying gas (N<sub>2</sub>) flow rate of 9 L min<sup>-1</sup>. Samples were analyzed in  
225 positive and negative mode separately; in each mode external mass calibration was  
226 conducted using Agilent low concentration tuning mix (part no. G1969-85000).  
227 Fragmentation spectra for specified ions were acquired across a range of collision  
228 energies (7-40 eV) in order to obtain good fragmentation spectra for as many ions as  
229 possible.

230

231 The purpose of the LC-TOF-MS<sup>2</sup> analysis was to allow high confidence assignment  
232 of molecular formulae to selected ions of interest identified by LC-IT-MS. This was  
233 achieved in two ways. Firstly, it provided more accurate *m/z* values for ions of interest  
234 for which the retention time was known, so constrained the number of corresponding  
235 peaks in the FT-ICR-MS spectra. FT-ICR-MS spectra of microlayer samples,

236 seawater samples and procedural blanks within this narrower  $m/z$  window were then  
237 compared to identify ions present at appropriate relative abundances, and possible  
238 molecular formulae for these were generated. Secondly, possible formulae for  
239 fragment ions and constant neutral losses detected by LC-TOF-MS<sup>2</sup> were used to  
240 identify relationships between groups of ions and inform formula selection. This  
241 information was combined with the FT-ICR-MS results in order to deduce probable  
242 molecular formulae for the target ions.

243

#### 244 **Supporting parameters**

245 The measurement of ice nucleating particles (INP) in untreated SML samples is  
246 described in Wilson et al., 2015. In order to determine whether INP were retained  
247 during the SPE extraction (Section 2.2), INP assays were also conducted on SML  
248 extracts that had been dried and reconstituted in a salt-water matrix (35 g L<sup>-1</sup>) and a  
249 matrix blank. The reconstitution volume was selected such that analyte concentrations  
250 were returned to those in the original, untreated SML sample. This allowed direct  
251 comparison of the extract IN activity with the microlayer IN activity measured in the  
252 raw samples during cruise JR288<sup>29</sup>.

253

254 Total organic carbon content of untreated SML samples was measured using a  
255 Shimadzu TOC-V analyzer, as described in Wilson et al., 2015. A suite of trace gases  
256 (DMS, halocarbons, monoterpenes) were measured by purge-and-trap gas  
257 chromatography mass spectrometry using the method described in<sup>55</sup>, though we  
258 caution that these results are semi-quantitative at best because microlayer sampling  
259 methods were not gas-tight.

260

261 **Results and discussion**

262

263 **Presence of microlayer enhanced ions revealed by LC-IT-MS**

264 Low mass resolution LC-IT-MS analysis of all samples revealed differences in  
265 organic composition, both between seawater and microlayer extracts, and within the  
266 subset of microlayer extracts. Total ion chromatograms obtained using LC-IT-MS  
267 showed a broad peak between 18 and 36 minutes in seawater and microlayer samples,  
268 while procedural blanks did not (Figs S1a, S2a). This broad peak is thought to be due  
269 to a large number of co-eluting, organic compounds present at low concentrations<sup>56</sup>.  
270 For some, but not all microlayer samples, discreet peaks appeared superimposed upon  
271 the broader hump (Figs S1a, S2a), suggesting a small number of ions either present at  
272 elevated levels, or with substantially higher ionization efficiencies. Base peak  
273 chromatograms (which display the abundance of the most intense ion in the mass  
274 spectra at each time point) confirmed the enhancement of selected ions in the  
275 microlayer (Figs S1b, S2b). In contrast, seawater samples did not exhibit any discreet  
276 peaks within this region.

277

278 Average mass spectra calculated for the 18-36 minute retention time region showed a  
279 characteristic distribution of peaks separated by 14 Da (corresponding to a CH<sub>2</sub> unit)  
280 for all seawater samples (Fig S3). Note that the choice of instrumental parameters  
281 (e.g. target mass) will influence the shape and center of the  $m/z$  distributions obtained,  
282 as well as the response factors of individual ions, so only data obtained under the  
283 same conditions can be directly compared. Average mass spectra were strikingly  
284 similar for all seawater samples, suggesting homogeneity in the extracted organic  
285 matter between sampling stations. Average mass spectra of microlayer samples

286 displayed additional peaks with higher relative intensity than observed in the seawater  
287 samples (Fig S3). This is consistent with the presence of elevated concentrations of  
288 certain ions in the microlayer compared to the underlying seawater.

289

290 LC-IT-MS chromatograms for microlayer sampling boat blanks did not contain these  
291 enhanced species, and the average mass spectra appeared similar to those for the  
292 seawater from which they were prepared (Figs S1, S2 and S3), suggesting they were  
293 not the result of contamination during microlayer sampling.

294

295 Inspection of base peak chromatograms and average mass spectra obtained by LT-IT-  
296 MS found 33 negative ions and 117 positive ions that were enhanced in microlayer  
297 samples, and these ions were selected for further study. Peak areas (obtained from  
298 extracted ion chromatograms) for these microlayer enhanced ions were normalized  
299 according to aqueous extraction volume, and used as a proxy for their relative  
300 abundances. As the sensitivity of ESI-MS varies across different compounds and as a  
301 function of matrix, peak areas are only used to compare the same ions (at same  
302 retention time and so approximately same matrix) across samples, and not to compare  
303 abundances of different ions within or between samples.

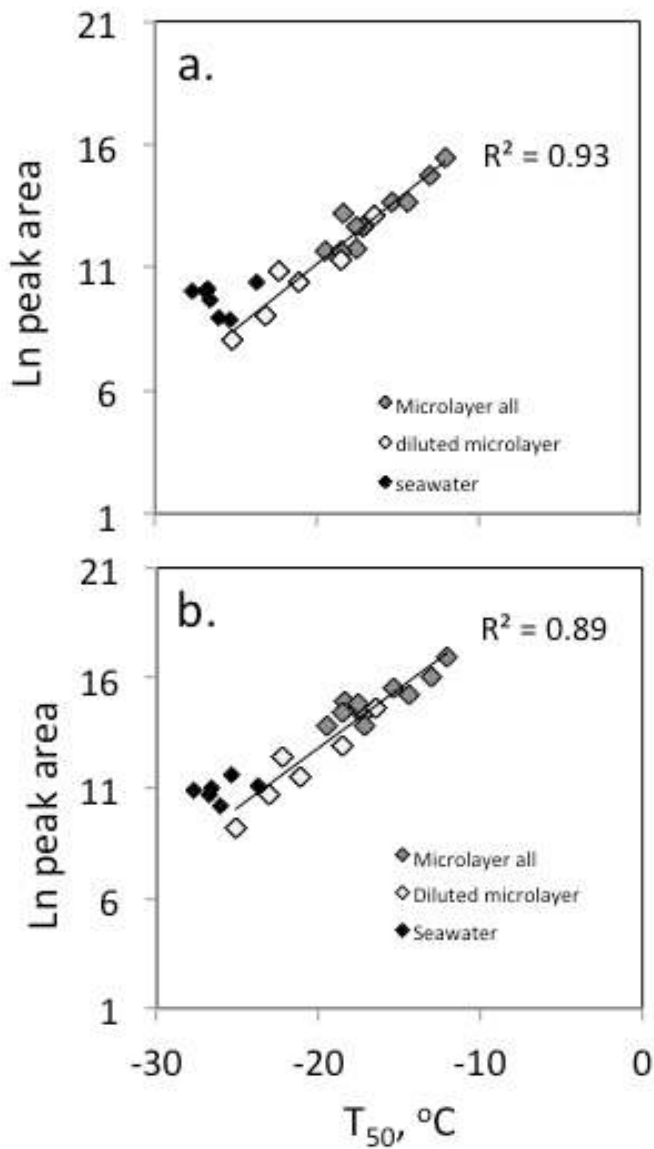
304

### 305 **Link between abundance of microlayer enhanced ions and ice nucleation activity**

306 The microlayer samples had higher ice nucleation (IN) activity than the underlying  
307 seawater, and this varied between stations (see Wilson et al., 2015). Ice nucleation  
308 ability, quantified in terms of median freezing temperature ( $T_{50}$ ; the temperature at  
309 which 50% of droplets had frozen), was correlated with the relative abundances of  
310 some of the microlayer enhanced ions identified by LC-IT-MS analysis (Fig 2, Table

311 1). Considering the microlayer samples only, linear correlation coefficients of  $R^2 >$   
312 0.5 were obtained for 7 negative ions and 27 positive ions (Table 1); for ease, these  
313 ions are referred to as 'IN tracer ions' hereafter. To examine this relationship over a  
314 wider linear range, correlation analysis was extended to include the measured IN  
315 activity of diluted microlayer samples (1% and 10% by volume) and calculated ion  
316 abundance, assuming that peak area scales linearly for the ions of interest. This  
317 revealed strong exponential relationships between IN activity and IN tracer ion  
318 relative abundance, with correlation coefficients of  $R^2 > 0.8$  in all but one case (Fig 2,  
319 Table 1). Seawater samples also appear to broadly fit this relationship (Fig 2), but  
320 were not included in quantitative correlation analysis as both ice nucleation ability  
321 and peak area were at or very close to the limit of detection.  
322





323

324

325 **Figure 2.** Natural log of volume normalized peak area plotted against 50% freezing  
 326 temperature, for ions with (a) retention time 30.8 mins, [M-H]<sup>-</sup> = 289.2 and (b)  
 327 retention time 38.5 mins, [M+H]<sup>+</sup> = 285.2 for microlayer (grey diamonds) and  
 328 seawater (black diamonds) samples, and microlayer samples diluted with ultrapure  
 329 water to 10 and 1% by volume (white diamonds). Lines of best fit and correlation  
 330 coefficients are for microlayer (whole and diluted) only, assuming peak area scales

331 linearly with sample dilution; seawater values were excluded from correlation  
332 analysis as they were at or close to the limit of detection for both ice nucleation ability  
333 and peak area.

334

335 The correlations between IN tracer ion abundance and  $T_{50}$  for microlayer samples are  
336 comparable or greater than that identified between  $T_{50}$  and TOC content of the  
337 microlayer ( $R^2 = 0.51$ ). For many ions, the relationship between ion abundance and  
338 IN activity was also stronger than that between ion abundance and TOC (Table 1).  
339 The IN tracer ions were variably correlated with TOC (Table 1), consistent with  
340 compositional differences between the SML samples, rather than solely a  
341 homogenous DOC pool present at varying concentrations.

342

343 IN assays of reconstituted SPE extracts yielded freezing curves that were very similar  
344 to those of the salt-water matrix (Fig. S4) and of the fresh seawater analyzed  
345 immediately following collection<sup>29</sup>. The elevated freezing temperatures characteristic  
346 of the raw microlayer samples<sup>29</sup> were not observed in the reconstituted SPE extracts.  
347 This implies that the INPs are not extracted and/or preserved by the SPE protocol, and  
348 that the IN tracer ions are only associated with INPs, but do not contribute directly to  
349 ice nucleation.

350

351

352

353

354

355 **Table 1.** Formula assignment, correlation coefficients ( $R^2$ ) and enrichment factors (EF) for ice nucleation tracer ions that were enhanced the  
 356 SML, in order of retention time ( $t_R$ ).

$t_R$ , mins	Mode	Exact m/z	Suggested formula	Formula error, ppm	Adduct	Fragment ions	$R^2$ Peak area vs. $T_{50}$	$R^2$ Ln(peak area) vs. $T_{50}^*$	$R^2$ Peak area vs. TOC	EF range
23.1	+	187.09647	C <sub>9</sub> H <sub>14</sub> O <sub>4</sub>	0.08	[M+H] <sup>+</sup>	b	0.56	0.87	0.62	12 - 436
23.9	+	273.13086	C <sub>11</sub> H <sub>22</sub> O <sub>6</sub>	-0.00	[M+Na] <sup>+</sup>	a	0.52	0.85	0.56	16 - 85
24.3	+	197.11723	C <sub>11</sub> H <sub>16</sub> O <sub>3</sub>	-0.05	[M+H] <sup>+</sup>	179.11, 161.10, (135), 133.10, 107.09, 93.07	0.55	0.84	0.85	29 - 1502
26.5	-	261.13429	C <sub>12</sub> H <sub>22</sub> O <sub>6</sub>	-0.27	[M-H] <sup>-</sup>	187.09, 125.09	0.52	0.85	0.52	2 - 175
28.6	+	285.13105 285.16727	C <sub>12</sub> H <sub>22</sub> O <sub>6</sub> C <sub>13</sub> H <sub>26</sub> O <sub>5</sub> C <sub>19</sub> H <sub>25</sub> S <sup>+</sup>	-0.65 -0.09 -0.43	[M+Na] <sup>+</sup> [M+Na] <sup>+</sup>	a	0.58	0.81	0.26	8 - 167
29.4	+	125.09606	C <sub>8</sub> H <sub>12</sub> O	0.25	[M+H] <sup>+</sup>	a	0.61	0.90	0.55	6 - 97
29.7	+	299.14675	C <sub>13</sub> H <sub>24</sub> O <sub>6</sub>	-0.80	[M+Na] <sup>+</sup>	73.6079	0.56	0.80	0.26	14 - 101
29.9	+	123.11685	C <sub>9</sub> H <sub>14</sub>	-0.19	[M+H] <sup>+</sup>	b	0.58	0.81	0.46	18 - 124

30.7	+	273.13086 273.16968	C <sub>11</sub> H <sub>22</sub> O <sub>6</sub> C <sub>14</sub> H <sub>24</sub> O <sub>5</sub>	0.00 -0.11	[M+Na] <sup>+</sup> [M+H] <sup>+</sup>	c	0.58	0.86	0.48	6 - 50
30.8	-	289.15757 289.16557	C <sub>14</sub> H <sub>27</sub> O <sub>4</sub> P C <sub>14</sub> H <sub>26</sub> O <sub>6</sub>	0.61 -0.31	[M-H] <sup>-</sup> [M-H] <sup>-</sup>	215.12	0.71	0.93	0.50	5 - 115
31.0	+	315.17790	C <sub>14</sub> H <sub>28</sub> O <sub>6</sub>	-0.30	[M+Na] <sup>+</sup>	a	0.52	0.81	0.42	28 - 272
31.5	-	187.13382	C <sub>10</sub> H <sub>20</sub> O <sub>3</sub>	-0.46	[M-H] <sup>-</sup>	167.10, 151.04, 141.12, 112.98	0.56	0.87	0.53	35 - 647
31.6	+	171.13797	C <sub>10</sub> H <sub>18</sub> O <sub>2</sub>	-0.08	[M+H] <sup>+</sup>	153.13, 135.12, 107.09	0.55	0.86	0.54	12 - 266
31.7	+	273.16968	C <sub>14</sub> H <sub>24</sub> O <sub>5</sub>	-0.11	[M+H] <sup>+</sup>	153.13, 135.12	0.57	0.81	0.39	11 - 399
31.8	-	289.15757 289.16557	C <sub>14</sub> H <sub>27</sub> O <sub>4</sub> P C <sub>14</sub> H <sub>26</sub> O <sub>6</sub>	0.61 -0.31	[M-H] <sup>-</sup> [M-H] <sup>-</sup>	215.12, 197.11	0.61	0.86	0.46	23 - 894
31.9	+	257.17489	C <sub>14</sub> H <sub>24</sub> O <sub>4</sub>	-0.60	[M+H] <sup>+</sup>	211.08, 147.12, 137.13, 95.09	0.52	0.82	0.60	3 - 326
33.9	+	187.13281	C <sub>10</sub> H <sub>18</sub> O <sub>3</sub>	0.33	[M+H] <sup>+</sup>	173.12, 155.11, 137.10, 119.09, 109.10, 95.09	0.53	0.86	0.57	41 - 744
34.0	+	241.14100	C <sub>11</sub> H <sub>22</sub> O <sub>4</sub>	-0.12	[M+Na] <sup>+</sup>	209.12	0.54	0.81	0.41	82 - 1952
35.7	+	241.14100	C <sub>11</sub> H <sub>22</sub> O <sub>4</sub>	0.12	[M+Na] <sup>+</sup>	209.12	0.58	0.85	0.68	15 - 273
36.6	+	167.14304	C <sub>11</sub> H <sub>18</sub> O	0.19	[M+H] <sup>+</sup>	149.13, 121.10, 109.10, 95.09, 81.07	0.57	0.87	0.72	162 -

										5512
36.7	-	201.14952	C <sub>11</sub> H <sub>22</sub> O <sub>3</sub>	0.49	[M-H] <sup>-</sup>	155.14	0.55	0.87	0.69	386 - 12931
36.7	+	149.13246	C <sub>11</sub> H <sub>16</sub>	0.11	[M+H] <sup>+</sup>	121.10, 109.10, 107.09, 95.09	0.56	0.87	0.69	17 - 625
36.7	+	185.15361	C <sub>11</sub> H <sub>20</sub> O <sub>2</sub>	-0.02	[M+H] <sup>+</sup>	167.14, 149.13, 121.10, 109.10, 95.09, 83.09, 81.07	0.56	0.87	0.71	86 - 1927
38.5	+	285.20581	C <sub>16</sub> H <sub>28</sub> O <sub>4</sub>	0.79	[M+H] <sup>+</sup>	b	0.66	0.89	0.53	17-67
39.1	+	125.13251	C <sub>9</sub> H <sub>16</sub>	-0.26	[M+H] <sup>+</sup>	c	0.52	0.87	0.67	9 - 114
39.2	-	236.11384	C <sub>20</sub> H <sub>42</sub> O <sub>8</sub> S <sub>2</sub>	-0.85	[M-2H] <sup>2-</sup>	375.24, 96.96	0.64	0.84	0.29	52 - 1944
40.1	-	236.11384	C <sub>20</sub> H <sub>42</sub> O <sub>8</sub> S <sub>2</sub>	-0.85	[M-2H] <sup>2-</sup>	375.24, 195.13, 154.06, 96.96	0.64	0.78	0.16	25 - 3728
40.7	+	257.17464	C <sub>14</sub> H <sub>24</sub> O <sub>4</sub>	-0.37	[M+H] <sup>+</sup>	201.15, 183.14, 165.13, 147.12, 137.13, 123.12, 95.09	0.53	0.84	0.49	8 - 244

357 Where two different  $m/z$  are listed, it was not possible to unambiguously identify the tracer ion in the FT-ICR-MS spectra. Where fragment ions  
358 are not given either (a) the ion did not fragment, (b) the fragmentation spectra were of very low intensity, or (c) the tracer ion was not apparent in  
359 the LC-TOF-MS<sup>2</sup> chromatogram. Rows shaded grey indicate formulae that are related to each other by the loss or gain of water molecules, so  
360 may indicate adducts of the same compound. Correlation coefficients are shown for relative abundance versus ice nucleation ability, measured as  
361 median freezing temperature ( $T_{50}$ ), and total organic carbon content (TOC). \*Correlation of Ln(peak area) against  $T_{50}$  includes diluted microlayer

362 samples. Enrichment factors are estimated as the ratio of the peak area in a microlayer sample to that in the corresponding seawater sample,  
363 following adjustment for extraction volume; the range for all microlayer samples is shown.

364 **Identity and potential origin of IN tracer ions**

365 Microlayer enhanced peaks (and high IN activity) were particularly common and  
366 abundant at station 12, and also stations 6, 12.5 and 19 (Figs S1, S2 and S3). The  
367 underlying water at stations 6, 12, 12.5 and 19 did not exhibit any distinctive features  
368 in either total or size-segregated chlorophyll concentrations (C. Hughes, University of  
369 York, unpub. data), or the chlorophyll contribution of individual phytoplankton  
370 groups derived from pigment analysis (A. Small, Oxford University, unpub. data).  
371 Similarly, there was no apparent relationship between the variation in SML  
372 composition (as determined here) or freezing temperature (as presented in Wilson et  
373 al.<sup>29</sup>) and the numbers of bacteria present (cell count data presented in Wilson et al.<sup>29</sup>).  
374 Examination of temperature-salinity profiles, and the shipboard wind speed and  
375 ambient light levels at the time of sampling, and in the 6 and 24 hours prior to the  
376 SML sampling, also failed to show any corresponding trends. Interestingly, semi-  
377 quantitative determinations of the biogenic trace gases dimethyl sulfide, methyl  
378 iodide, bromochloromethane and di-iodomethane revealed that these gases also  
379 tended to be present at higher levels in microlayer samples 6, 12, 12.5 and 19 than in  
380 other samples (Fig S5). These stations were also unusual in that ethyl and propyl  
381 iodide were observed. From the above consideration of the available supporting  
382 evidence, a single factor associated with the relative abundance of IN tracer ions (and  
383 high INPs themselves) cannot be identified, but the associations with TOC and  
384 biogenic trace gases point towards a biological and/or photochemical influence.

385

386 The nature of marine INPs has not yet been fully elucidated, but evidence suggests  
387 they originate from marine phytoplankton or bacteria<sup>60-64</sup>. Phytoplankton cell exudates  
388 and/or cellular fragments, and the bacterial populations sustained by this material,

389 have both been suggested as possible sources<sup>29, 36, 63</sup>. Laboratory mesocosm  
390 experiments found that peaks in airborne IN activity coincided with increases in  
391 relatively aliphatic rich, low O/C organic material in submicron SSA; these changes  
392 were ascribed to phytoplankton cell lysis under conditions of relatively low bacterial  
393 lipase activity<sup>36, 64, 65</sup>. Cell breakage may occur in the surface ocean, with subsequent  
394 concentration of the products in the SML, or the process may be enhanced in the SML  
395 itself. Enrichments of mannose and arabinose in the SML have previously been  
396 attributed to phytoplankton cell degradation<sup>66</sup>. Aller et al.<sup>67</sup> observed an increased  
397 proportion of membrane damaged cells in the SML, and suggested this might be due  
398 to the increased potential for viral infection, zooplankton grazing and physical  
399 stresses in the microlayer. Either process could potentially result in increased  
400 abundances of INPs and other biogenic material in the SML. We hypothesize that the  
401 IN tracer ions originate from a phytoplankton exudate mix (including any associated  
402 bacteria and viruses), of which larger sized constituents confer the IN activity.

403

404 Phytoplankton are known to release a wide variety of organic compounds, ranging in  
405 size from volatile gases of less than 100 Da to macromolecules and colloids of several  
406 1000 Da. As a result of sample processing and instrumental constraints, this study  
407 (and all others using similar approaches), considers only an operationally defined  
408 fraction of the total organic matter present. Specifically, the analytical approaches  
409 used here have targeted compounds that are low molecular weight (<1000  $m/z$ ), water  
410 soluble, neither strongly hydrophobic or strongly hydrophilic, and easily ionizable by  
411 electrospray. High-resolution mass spectrometry was used to elucidate molecular  
412 formulae for the IN tracer ions (Table 1). Searches of online databases (e.g.  
413 Chemspider, MassBank, NIST) typically returned tens of structural isomers per



414 formula or more. Our data is insufficient to distinguish between these isomers, so we  
415 can only explore whether the IN formulae are consistent with algal exudates. For  
416 example, known algal metabolites with similar carbon numbers to the IN tracer ions  
417 include polyunsaturated aldehydes (PUAs; e.g. decatrienal,  $C_{10}H_{14}O$ )<sup>68</sup> and  
418 unsaturated hydrocarbons (e.g. fucoserratene,  $C_8H_{12}$ ; dictyopterenes,  $C_{11}H_{18}$ )<sup>69</sup>. Two  
419 tracer ion formulae exactly match those of compounds from these classes: isomers of  
420  $C_8H_{12}O$  include the PUA octadienal, while those of  $C_{11}H_{16}$  include the algal hormone  
421 hormosirene<sup>70</sup>. Other tracer ions have formulae consistent with oxygenated organics  
422 (e.g.  $C_8H_{14}O_3$ ,  $C_{12}H_{16}O_3$ ) formed when PUAs are produced by the cleavage of higher  
423 molecular weight polyunsaturated fatty acids (PUFA)<sup>71</sup>. PUAs are mainly produced  
424 by diatoms, as a response to cell wounding, for example by zooplankton grazing<sup>72</sup>;  
425 the elevated levels of DMS (and potentially halocarbons) observed in the samples  
426 with high levels of the IN tracer ions are indicative of grazing having taken place at  
427 these locations<sup>73</sup>. It is beyond the scope of this work to prove that the IN tracer ions  
428 were indeed derived from PUAs, but we speculate that cellular damage (e.g. by  
429 grazing, stress or viral infection) could cause the simultaneous release of PUAs, trace  
430 gases and INPs.

431

432 The IN tracer ions were massively enriched in the SML, with enrichment factors  
433 ranging from ~2 to 12931 (Table 1). Such EF values are several orders of magnitude  
434 greater than observed for dissolved organic carbon and other organic molecules<sup>12</sup>,  
435 supporting the possibility that the tracer ions were formed *in-situ*. One possible  
436 mechanism for this is the photo-chemical modification of organic matter within the  
437 SML. Many have formulae consistent with fatty acid and dicarboxylic acid groups,  
438 e.g. saturated oxo-fatty acids ( $C_nH_{2n-2}O_3$ ), and unsaturated dicarboxylic acids ( $C_nH_{2n-}$

439  $_4\text{O}_4$ ), which have been tentatively identified in nascent sea spray aerosol<sup>74</sup>.  
440 Compounds of these classes, including nine with identical formulae to the IN tracer  
441 ions, have been found to increase in abundance following the irradiation of cellular  
442 material from freshwater aquatic biofilms<sup>75</sup>. More generally, the photochemical  
443 production of low molecular weight, saturated and unsaturated, carbonyl compounds  
444 has been demonstrated in natural microlayer samples and model systems<sup>4, 5, 16, 76</sup>.  
445 Alternative oxidation mechanisms include the oxidation of unsaturated organic  
446 compounds by ozone at the air-sea interface<sup>77</sup>, or bacterial metabolism in the SML<sup>1, 28</sup>.  
447 Formation of the IN tracer ions within the SML by abiotic reactions or bacterial  
448 breakdown is not incompatible with a link to phytoplankton described above, as this  
449 may supply the precursor material.

450

#### 451 **Semi-quantitative comparison of seawater and microlayer SPE-DOM** 452 **composition using FT-ICR-MS**

453 Mass spectra obtained using the high resolution FT-ICR-MS echoed the general  
454 trends suggested by the LC-IT-MS analysis, described earlier. Seawater samples were  
455 similar across stations, even at the fine scale. The negative mode high-resolution mass  
456 spectra for seawater samples visually resemble those obtained in other studies<sup>22, 47, 57,</sup>  
457 <sup>58</sup>. As mentioned earlier, it should be noted that relative ion intensities across the  $m/z$   
458 range scanned are in part a function of user selected instrument settings. Previous  
459 studies have also reported a high level of homogeneity between SPE-DOM mass  
460 spectra for surface seawater samples<sup>57, 58</sup>.

461

462 In contrast, SML samples displayed differences both from seawater and each other,  
463 but boat blanks were very similar to those for seawater (Fig S6). The SML spectra

464 tended to contain peaks across a wider  $m/z$  range than the seawater spectra, and have  
465 more high intensity spikes. In the negative mode, higher molecular weight peaks ( $m/z$   
466  $\sim$ 700 to 900) were particularly prominent in SML samples 6 and 12.5, which also had  
467 high IN activity.

468

469 The visual contrast between seawater and SML spectra resembles the differences  
470 observed between ESI-FT-ICR mass spectra of underlying seawater and SML from an  
471 estuary, where enhancement of surfactant peaks has been observed<sup>22</sup>. Interestingly,  
472 seawater samples incubated with different microbial communities have also been  
473 shown to exhibit comparable differences in low molecular weight DOM  
474 composition<sup>59</sup>. In that study, plankton larger than  $\sim 1 \mu\text{m}$  were removed from  
475 seawater, resulting in a microbial community dominated by heterotopic bacteria.  
476 High-resolution mass spectra from these incubations revealed the presence of unique,  
477 high-abundance ions that were not present in spectra from whole water, and overall  
478 had higher average H/C ratios and lower DBE values<sup>59</sup>. In light of these findings, it  
479 seems plausible that differences in the DOM composition of the microlayer relative to  
480 seawater observed here could, at least in part, reflect the differing microbial  
481 communities in each.

482

483 In the positive mode LC-IT-MS average spectra, there is some indication that the  
484 microlayer may be depleted in compounds at the higher molecular weight end of the  
485 detection envelope ( $m/z$  200-400; Fig S2) relative to seawater. This is in agreement  
486 with the shift to smaller molecular size in the microlayer observed by Lechtenfeld et  
487 al.<sup>22</sup>, which was attributed to photochemical and microbiological degradation.  
488 Meanwhile, negative mode FT-ICR-MS spectra obtained by direct injection also

489 suggested the presence of additional higher molecular weight ( $m/z \sim 700$  to 900) peaks  
490 in some SML samples that were absent from seawater (Fig S6). These peaks were not  
491 present in the LC-IT-MS average mass spectra (Supp info Fig S3A), probably because  
492 they have long retention times and did not elute in the time window of interest.

493

494 Assignment of molecular formulae to negatively charged ions detected by FT-ICR-  
495 MS is described in the SI. Formula assignment for complex organic mixtures, where  
496 multiple heteratoms must be considered, can be ambiguous<sup>78,79</sup>, and we consider our  
497 results to be subject to uncertainty. Average DBE values and H/C ratios suggested  
498 SPE-DOM from the microlayer was slightly more aliphatic than that from seawater  
499 (Table S2). A tendency towards higher saturation and decreased aromaticity in the  
500 microlayer relative to the underlying seawater has been observed previously<sup>19,22</sup>, and  
501 is consistent with the enhancement of hydrophobic substances in the microlayer. That  
502 the SML was more aliphatic than the underlying water, and also had higher IN  
503 activity, is consistent with the observation of an association between IN activity and  
504 more aliphatic material in SSA<sup>36,64,65</sup>. However, we did not observe trends in average  
505 elemental ratios or DBE values within the SML subset that co-varied with IN  
506 activity.

507

#### 508 **Possible occurrence of SML derived compounds in atmospheric aerosol**

509 The presence of relatively low molecular weight, highly oxygenated compounds in  
510 the sea surface microlayer, raises the possibility that primary sea spray aerosol may  
511 also contribute to the atmospheric aerosol burden of such compounds in the marine  
512 environment. FT-ICR-MS identified ions with the same molecular formulae as five of  
513 the negatively charged IN tracer ions (Table 1) in ambient atmospheric aerosol

514 sampled in the Greenland Sea during the July-August 2013, but not March 2013  
515 (Table S3). Good agreement between observed spectra and simulated isotopic patterns  
516 (indicated by a relatively low mSigma value) confirmed that the molecular formulae  
517 agreed. These ions were absent from the aerosol sampling procedural blanks. The  
518 possible occurrence of IN tracer ions in ambient atmospheric aerosol is consistent  
519 with the transfer of material, possibly including INPs, from the microlayer to sea  
520 spray aerosol. It has recently been demonstrated that SSA produced by wave breaking  
521 contains INPs at levels in agreement with ambient INP measurements made over the  
522 oceans<sup>36</sup>. That the IN tracer ions were only found in aerosol collected during the  
523 summer, and not the early spring, is consistent with a biological source for these ions.

524

525

526

## 527 **Acknowledgements**

528 We acknowledge funding from the NERC ACCACIA (Aerosol-Cloud Coupling And  
529 Climate Interactions in the Arctic) project (NE/I028769/1), and are grateful to the  
530 Principal Investigator Prof Ian Brooks and to the cast and crew of the R/V *Lance*  
531 March 2013 and JR288 July 2013 cruises. The York Centre of Excellence in Mass  
532 Spectrometry was created thanks to a major capital investment through Science City  
533 York, supported by Yorkshire Forward with funds from the Northern Way Initiative.  
534 We thank Ed Bergström and David Ashford for assistance with FT-ICR-MS and  
535 maXis LT-TOF-MS<sup>2</sup> analyses respectively. The authors gratefully acknowledge the  
536 NOAA Air Resources Laboratory (ARL) for the provision of the HYSPLIT transport  
537 and dispersion model and/or READY website (<http://www.ready.noaa.gov>) used in  
538 this publication.

539

540 **Supporting information.** The FT-ICR-MS formula assignment procedure is  
541 described in the SI. Table S1 contains microlayer (and seawater) sampling  
542 information, and Table S2 contains average elemental composition information  
543 derived from FT-ICR-MS analysis of these samples. Table S3 provides details of  
544 aerosol sample collection, air mass origin and presence/absence of IN tracer ions.  
545 Total ion and base peak chromatograms obtained by LC-IT-MS for all samples are  
546 shown in Figures S1 and S2, and average mass spectra from these analyses are  
547 compared in Figure S3. Figure S4 shows freezing curves for reconstituted microlayer  
548 extracts, and raw microlayer and seawater extracts. Figure S5 compares the relative  
549 abundance of selected IN tracer ions with approximate concentrations of trace gases  
550 in microlayer samples. Negative mode FT-ICR mass spectra for seawater, microlayer  
551 and procedural blanks are shown in Figure S6, numbers of molecular formulae found  
552 in each sample type are given in Figure S7 (Venn diagram), and Figure S8 is a van  
553 Krevelen plot of these results. This information is available free of charge via the  
554 Internet at <http://pubs.acs.org>.

555  
556

## 557 **References**

558

- 559 1. Cunliffe, M.; Engel, A.; Frka, S.; Gasparovic, B.; Guitart, C.; Murrell, J. C.;  
560 Salter, M.; Stolle, C.; Upstill-Goddard, R.; Wurl, O. Sea surface microlayers: A  
561 unified physicochemical and biological perspective of the air-ocean interface.  
562 *Prog. Oceanogr.* **2013**, *109*, 104-116.
- 563 2. Wurl, O.; Wurl, E.; Miller, L.; Johnson, K.; Vagle, S. Formation and global  
564 distribution of sea-surface microlayers. *Biogeosciences* **2011**, *8* (1), 121-135.
- 565 3. Sabbaghzadeh, B.; Upstill-Goddard, R. C.; Beale, R.; Pereira, R.; Nightingale,  
566 P. D. The Atlantic Ocean surface microlayer from 50 degrees N to 50 degrees S is  
567 ubiquitously enriched in surfactants at wind speeds up to 13ms(-1). *Geophys.*  
568 *Res. Lett.* **2017**, *44* (6), 2852-2858.
- 569 4. Ciuraru, R.; Fine, L.; van Pinxteren, M.; D'Anna, B.; Herrmann, H.; George,  
570 C. Unravelling New Processes at Interfaces: Photochemical Isoprene Production  
571 at the Sea Surface. *Environ. Sci. Technol.* **2015**, *49* (22), 13199-13205.

- 572 5. Ciuraru, R.; Fine, L.; van Pinxteren, M.; D'Anna, B.; Herrmann, H.; George,  
573 C. Photosensitized production of functionalized and unsaturated organic  
574 compounds at the air-sea interface. *Scientific Reports* **2015**, *5*.
- 575 6. Ebling, A. M.; Landing, W. M. Sampling and analysis of the sea surface  
576 microlayer for dissolved and particulate trace elements. *Mar. Chem.* **2015**, *177*,  
577 134-142.
- 578 7. Shaw, M. D.; Carpenter, L. J. Modification of Ozone Deposition and I-2  
579 Emissions at the Air-Aqueous Interface by Dissolved Organic Carbon of Marine  
580 Origin. *Environ. Sci. Technol.* **2013**, *47* (19), 10947-10954.
- 581 8. del Vento, S.; Dachs, J. Influence of the surface microlayer on atmospheric  
582 deposition of aerosols and polycyclic aromatic hydrocarbons. *Atmos. Environ.*  
583 **2007**, *41* (23), 4920-4930.
- 584 9. Frew, N. M.; Bock, E. J.; Schimpf, U.; Hara, T.; Haussecker, H.; Edson, J. B.;  
585 McGillis, W. R.; Nelson, R. K.; McKenna, S. P.; Uz, B. M.; Jahne, B. Air-sea gas  
586 transfer: Its dependence on wind stress, small-scale roughness, and surface films.  
587 *J. Geophys. Res.: Oceans* **2004**, *109* (C8), 23.
- 588 10. Donaldson, D. J.; George, C. Sea-Surface Chemistry and Its Impact on the  
589 Marine Boundary Layer. *Environ. Sci. Technol.* **2012**, *46* (19), 10385-10389.
- 590 11. Blanchard, D. C. Sea-to-air transport of surface active material. *Science*  
591 **1964**, *146* (364), 396-&.
- 592 12. Quinn, P. K.; Collins, D. B.; Grassian, V. H.; Prather, K. A.; Bates, T. S.  
593 Chemistry and Related Properties of Freshly Emitted Sea Spray Aerosol. *Chem.*  
594 *Rev.* **2015**, *115* (10), 4383-4399.
- 595 13. Leck, C.; Bigg, E. K. Biogenic particles in the surface microlayer and  
596 overlaying atmosphere in the central Arctic Ocean during summer. *Tellus Series*  
597 *B-Chemical and Physical Meteorology* **2005**, *57* (4), 305-316.
- 598 14. Roslan, R. N.; Hanif, N. M.; Othman, M. R.; Azmi, W.; Yan, X. X.; Ali, M. M.;  
599 Mohamed, C. A. R.; Latif, M. T. Surfactants in the sea-surface microlayer and their  
600 contribution to atmospheric aerosols around coastal areas of the Malaysian  
601 peninsula. *Marine Pollution Bulletin* **2010**, *60* (9), 1584-1590.
- 602 15. Mungall, E. L.; Abbatt, J. P. D.; Wentzell, J. J. B.; Lee, A. K. Y.; Thomas, J. L.;  
603 Blais, M.; Gosselin, M.; Miller, L. A.; Papakyriakou, T.; Willis, M. D.; Liggio, J.  
604 Microlayer source of oxygenated volatile organic compounds in the summertime  
605 marine Arctic boundary layer. *Proc. Natl. Acad. Sci. U.S.A.* **2017**, *114* (24), 6203-  
606 6208.
- 607 16. Zhou, X. L.; Mopper, K. Photochemical production of low-molecular-  
608 weight carbonyl compounds in seawater and surface microlayer and their air-sea  
609 exchange. *Mar. Chem.* **1997**, *56* (3-4), 201-213.
- 610 17. van Pinxteren, M.; Muller, C.; Iinuma, Y.; Stolle, C.; Herrmann, H. Chemical  
611 Characterization of Dissolved Organic Compounds from Coastal Sea Surface  
612 Micro layers (Baltic Sea, Germany). *Environ. Sci. Technol.* **2012**, *46* (19), 10455-  
613 10462.
- 614 18. Antonowicz, J. P. Daily cycle of variability contents of phosphorus forms in  
615 surface microlayer of a light salinity Baltic Sea Lagoon lake (North Poland) - Part  
616 II. *Central European Journal of Chemistry* **2013**, *11* (5), 817-826.
- 617 19. Calace, N.; Mirante, S.; Petronio, B. M.; Pietroletti, M.; Rugo, C. Fulvic acid  
618 enrichment in the microlayer of the Gerlache Inlet sea (Antarctica): Preliminary  
619 results. *International Journal of Environmental Analytical Chemistry* **2004**, *84* (6-  
620 7), 413-421.

- 621 20. Garcia-Flor, N.; Guitart, C.; Abalos, M.; Dachs, J.; Bayona, J. M.; Albaiges, J.  
622 Enrichment of organochlorine contaminants in the sea surface microlayer: An  
623 organic carbon-driven process. *Mar. Chem.* **2005**, *96* (3-4), 331-345.
- 624 21. Hardy, J. T.; Cleary, J. Surface microlayer contamination and toxicity in the  
625 German Bight. *Mar. Ecol. Prog. Ser.* **1992**, *91* (1-3), 203-210.
- 626 22. Lechtenfeld, O. J.; Koch, B. P.; Gasparovic, B.; Frka, S.; Witt, M.; Kattner, G.  
627 The influence of salinity on the molecular and optical properties of surface  
628 microlayers in a karstic estuary. *Mar. Chem.* **2013**, *150*, 25-38.
- 629 23. Galgani, L.; Piontek, J.; Engel, A. Biopolymers form a gelatinous microlayer  
630 at the air-sea interface when Arctic sea ice melts. *Scientific Reports* **2016**, *6*, 10.
- 631 24. Cincinelli, A.; Stortini, A. M.; Perugini, M.; Checchini, L.; Lepri, L. Organic  
632 pollutants in sea-surface microlayer and aerosol in the coastal environment of  
633 Leghorn - (Tyrrhenian Sea). *Mar. Chem.* **2001**, *76* (1-2), 77-98.
- 634 25. Jayarathne, T.; Sultana, C. M.; Lee, C.; Malfatti, F.; Cox, J. L.; Pendergraft, M.  
635 A.; Moore, K. A.; Azam, F.; Tivanski, A. V.; Cappa, C. D.; Bertram, T. H.; Grassian, V.  
636 H.; Prather, K. A.; Stone, E. A. Enrichment of Saccharides and Divalent Cations in  
637 Sea Spray Aerosol During Two Phytoplankton Blooms. *Environ. Sci. Technol.*  
638 **2016**, *50* (21), 11511-11520.
- 639 26. Gao, Q.; Leck, C.; Rauschenberg, C.; Matrai, P. A. On the chemical dynamics  
640 of extracellular polysaccharides in the high Arctic surface microlayer. *Ocean*  
641 *Science* **2012**, *8* (4), 401-418.
- 642 27. Kuznetsova, M.; Lee, C.; Aller, J. Characterization of the proteinaceous  
643 matter in marine aerosols. *Mar. Chem.* **2005**, *96* (3-4), 359-377.
- 644 28. Kuznetsova, M.; Lee, C. Enhanced extracellular enzymatic peptide  
645 hydrolysis in the sea-surface microlayer. *Mar. Chem.* **2001**, *73* (3-4), 319-332.
- 646 29. Wilson, T. W.; Ladino, L. A.; Alpert, P. A.; Breckels, M. N.; Brooks, I. M.;  
647 Browse, J.; Burrows, S. M.; Carslaw, K. S.; Huffman, J. A.; Judd, C.; Kilhau, W. P.;  
648 Mason, R. H.; McFiggans, G.; Miller, L. A.; Najera, J. J.; Polishchuk, E.; Rae, S.;  
649 Schiller, C. L.; Si, M.; Temprado, J. V.; Whale, T. F.; Wong, J. P. S.; Wurl, O.; Yakobi-  
650 Hancock, J. D.; Abbatt, J. P. D.; Aller, J. Y.; Bertram, A. K.; Knopf, D. A.; Murray, B. J.  
651 A marine biogenic source of atmospheric ice-nucleating particles. *Nature* **2015**,  
652 *525* (7568), 234-.
- 653 30. Bigg, E. K. Ice nucleus concentrations in remote areas. *Journal of the*  
654 *Atmospheric Sciences* **1973**, *30* (6), 1153-1157.
- 655 31. Bigg, E. K. Ice forming nuclei in the high Arctic. *Tellus Series B-Chemical*  
656 *and Physical Meteorology* **1996**, *48* (2), 223-233.
- 657 32. Schnell, R. C. Ice nuclei in seawater, fog water and marine air off the coast  
658 of Nova-Scotia - summer 1975. *Journal of the Atmospheric Sciences* **1977**, *34* (8),  
659 1299-1305.
- 660 33. Schnell, R. C.; Vali, G. Freezing nuclei in marine waters. *Tellus* **1975**, *27*  
661 (3), 321-323.
- 662 34. Schnell, R. C.; Vali, G. Biogenic ice nuclei. 1. Terrestrial and marine  
663 sources. *Journal of the Atmospheric Sciences* **1976**, *33* (8), 1554-1564.
- 664 35. Rosinski, J.; Haagenson, P. L.; Nagamoto, C. T.; Parungo, F. Nature of ice-  
665 forming nuclei in marine air masses. *Journal of Aerosol Science* **1987**, *18* (3), 291-  
666 .
- 667 36. DeMott, P. J.; Hill, T. C. J.; McCluskey, C. S.; Prather, K. A.; Collins, D. B.;  
668 Sullivan, R. C.; Ruppel, M. J.; Mason, R. H.; Irish, V. E.; Lee, T.; Hwang, C. Y.; Rhee, T.  
669 S.; Snider, J. R.; McMeeking, G. R.; Dhaniyala, S.; Lewis, E. R.; Wentzell, J. J. B.;



670 Abbatt, J.; Lee, C.; Sultana, C. M.; Ault, A. P.; Axson, J. L.; Martinez, M. D.; Venero, I.;  
671 Santos-Figueroa, G.; Stokes, M. D.; Deane, G. B.; Mayol-Bracero, O. L.; Grassian, V.  
672 H.; Bertram, T. H.; Bertram, A. K.; Moffett, B. F.; Franc, G. D. Sea spray aerosol as a  
673 unique source of ice nucleating particles. *Proc. Natl. Acad. Sci. U.S.A.* **2016**, *113*  
674 (21), 5797-5803.

675 37. Burrows, S. M.; Hoose, C.; Poschl, U.; Lawrence, M. G. Ice nuclei in marine  
676 air: biogenic particles or dust? *Atmos. Chem. Phys.* **2013**, *13* (1), 245-267.

677 38. Vergara-Temprado, J.; Murray, B. J.; Wilson, T. W.; O'Sullivan, D.; Browse,  
678 J.; Pringle, K. J.; Ardon-Dryer, K.; Bertram, A. K.; Burrows, S. M.; Ceburnis, D.;  
679 DeMott, P. J.; Mason, R. H.; O'Dowd, C. D.; Rinaldi, M.; Carslaw, K. S. Contribution  
680 of feldspar and marine organic aerosols to global ice nucleating particle  
681 concentrations. *Atmos. Chem. Phys.* **2017**, *17* (5), 3637-3658.

682 39. Knulst, J. C.; Rosenberger, D.; Thompson, B.; Paatero, J. Intensive sea  
683 surface microlayer investigations of open leads in the pack ice during Arctic  
684 Ocean 2001 expedition. *Langmuir* **2003**, *19* (24), 10194-10199.

685 40. Schlitzer, R. *Ocean Data View*, <http://odv.awi.de>: 2014.

686 41. Dittmar, T.; Koch, B.; Hertkorn, N.; Kattner, G. A simple and efficient  
687 method for the solid-phase extraction of dissolved organic matter (SPE-DOM)  
688 from seawater. *Limnology and Oceanography-Methods* **2008**, *6*, 230-235.

689 42. Longnecker, K. Dissolved organic matter in newly formed sea ice and  
690 surface seawater. *Geochim. Cosmochim. Acta* **2015**, *171*, 39-49.

691 43. McIntyre, C.; McRae, C. Proposed guidelines for sample preparation and  
692 ESI-MS analysis of humic substances to avoid self-esterification. *Organic*  
693 *Geochemistry* **2005**, *36* (4), 543-553.

694 44. Bateman, A. P.; Walser, M. L.; Desyaterik, Y.; Laskin, J.; Laskin, A.;  
695 Nizkorodov, S. A. The effect of solvent on the analysis of secondary organic  
696 aerosol using electrospray ionization mass spectrometry. *Environ. Sci. Technol.*  
697 **2008**, *42* (19), 7341-7346.

698 45. Flerus, R.; Koch, B. P.; Schmitt-Kopplin, P.; Witt, M.; Kattner, G. Molecular  
699 level investigation of reactions between dissolved organic matter and extraction  
700 solvents using FT-ICR MS. *Mar. Chem.* **2011**, *124* (1-4), 100-107.

701 46. Stein, A. F.; Draxler, R. R.; Rolph, G. D.; Stunder, B. J. B.; Cohen, M. D.; Ngan,  
702 F. NOAA's HYSPLIT atmospheric transport and dispersion modeling system.  
703 *Bulletin American Meteorological Society* **2015**, *96*, 2059-2077.

704 47. Kujawinski, E. B.; Longnecker, K.; Blough, N. V.; Del Vecchio, R.; Finlay, L.;  
705 Kitner, J. B.; Giovannoni, S. J. Identification of possible source markers in marine  
706 dissolved organic matter using ultrahigh resolution mass spectrometry. *Geochim.*  
707 *Cosmochim. Acta* **2009**, *73* (15), 4384-4399.

708 48. Hertkorn, N.; Harir, M.; Koch, B. P.; Michalke, B.; Schmitt-Kopplin, P. High-  
709 field NMR spectroscopy and FTICR mass spectrometry: powerful discovery tools  
710 for the molecular level characterization of marine dissolved organic matter.  
711 *Biogeosciences* **2013**, *10* (3), 1583-1624.

712 49. Hawkes, J. A.; Hansen, C. T.; Goldhammer, T.; Bach, W.; Dittmar, T.  
713 Molecular alteration of marine dissolved organic matter under experimental  
714 hydrothermal conditions. *Geochim. Cosmochim. Acta* **2016**, *175*, 68-85.

715 50. Schmitt-Kopplin, P.; Liger-Belair, G.; Koch, B. P.; Flerus, R.; Kattner, G.;  
716 Harir, M.; Kanawati, B.; Lucio, M.; Tziotis, D.; Hertkorn, N.; Gebefugi, I. Dissolved  
717 organic matter in sea spray: a transfer study from marine surface water to  
718 aerosols. *Biogeosciences* **2012**, *9* (4), 1571-1582.

719 51. Stubbins, A.; Spencer, R. G. M.; Chen, H. M.; Hatcher, P. G.; Mopper, K.;  
720 Hernes, P. J.; Mwamba, V. L.; Mangangu, A. M.; Wabakanghanzi, J. N.; Six, J.  
721 Illuminated darkness: Molecular signatures of Congo River dissolved organic  
722 matter and its photochemical alteration as revealed by ultrahigh precision mass  
723 spectrometry. *Limnol. Oceanogr.* **2010**, *55* (4), 1467-1477.

724 52. Gurganus, S. C.; Wozniak, A. S.; Hatcher, P. G. Molecular characteristics of  
725 the water soluble organic matter in size-fractionated aerosols collected over the  
726 North Atlantic Ocean. *Mar. Chem.* **2015**, *170*, 37-48.

727 53. Kujawinski, E. B.; Behn, M. D. Automated analysis of electrospray  
728 ionization Fourier transform ion cyclotron resonance mass spectra of natural  
729 organic matter. *Anal. Chem.* **2006**, *78* (13), 4363-4373.

730 54. Wozniak, A. S.; Bauer, J. E.; Sleighter, R. L.; Dickhut, R. M.; Hatcher, P. G.  
731 Technical Note: Molecular characterization of aerosol-derived water soluble  
732 organic carbon using ultrahigh resolution electrospray ionization Fourier  
733 transform ion cyclotron resonance mass spectrometry. *Atmos. Chem. Phys.* **2008**,  
734 *8* (17), 5099-5111.

735 55. Andrews, S. J.; Hackenberg, S. C.; Carpenter, L. J. Technical Note: A fully  
736 automated purge and trap GC-MS system for quantification of volatile organic  
737 compound (VOC) fluxes between the ocean and atmosphere. *Ocean Sci.* **2015**, *11*  
738 (2), 313-321.

739 56. Dittmar, T.; Whitehead, K.; Minor, E. C.; Koch, B. P. Tracing terrigenous  
740 dissolved organic matter and its photochemical decay in the ocean by using  
741 liquid chromatography/mass spectrometry. *Mar. Chem.* **2007**, *107* (3), 378-387.

742 57. Flerus, R.; Lechtenfeld, O. J.; Koch, B. P.; McCallister, S. L.; Schmitt-Kopplin,  
743 P.; Benner, R.; Kaiser, K.; Kattner, G. A molecular perspective on the ageing of  
744 marine dissolved organic matter. *Biogeosciences* **2012**, *9* (6), 1935-1955.

745 58. Gonsior, M.; Peake, B. M.; Cooper, W. T.; Podgorski, D. C.; D'Andrilli, J.;  
746 Dittmar, T.; Cooper, W. J. Characterization of dissolved organic matter across the  
747 Subtropical Convergence off the South Island, New Zealand. *Mar. Chem.* **2011**,  
748 *123* (1), 99-110.

749 59. Kujawinski, E. B.; Longnecker, K.; Barott, K. L.; Weber, R. J. M.; Kido Soule,  
750 M. C. Microbial Community Structure Affects Marine Dissolved Organic Matter  
751 Composition. *Frontiers in Marine Science* **2016**, *3* (45).

752 60. Knopf, D. A.; Alpert, P. A.; Wang, B.; Aller, J. Y. Stimulation of ice nucleation  
753 by marine diatoms. *Nat. Geosci.* **2011**, *4* (2), 88-90.

754 61. Schnell, R. C. Ice nuclei produced by laboratory cultured marine  
755 phytoplankton. *Geophys. Res. Lett.* **1975**, *2* (11), 500-502.

756 62. Fall, R.; Schnell, R. C. Association of an ice-nucleating pseudomonad with  
757 cultures of the marine dinoflagellate, *Heterocapsa niei*. *J. Mar. Res.* **1985**, *43* (1),  
758 257-265.

759 63. Ladino, L. A.; Yakobi-Hancock, J. D.; Kilhau, W. P.; Mason, R. H.; Si, M.; Li,  
760 J.; Miller, L. A.; Schiller, C. L.; Huffman, J. A.; Aller, J. Y.; Knopf, D. A.; Bertram, A. K.;  
761 Abbatt, J. P. D. Addressing the ice nucleating abilities of marine aerosol: A  
762 combination of deposition mode laboratory and field measurements. *Atmos.*  
763 *Environ.* **2016**, *132*, 1-10.

764 64. McCluskey, C. S.; Hill, T. C. J.; Malfatti, F.; Sultana, C. M.; Lee, C.; Santander,  
765 M. V.; Beall, C. M.; Moore, K. A.; Cornwell, G. C.; Collins, D. B.; Prather, K. A.;  
766 Jayarathne, T.; Stone, E. A.; Azam, F.; Kreidenweis, S. M.; DeMott, P. J. A Dynamic  
767 Link between Ice Nucleating Particles Released in Nascent Sea Spray Aerosol and

768 Oceanic Biological Activity during Two Mesocosm Experiments. *Journal of the*  
769 *Atmospheric Sciences* **2017**, *74* (1), 151-166.  
770 65. Wang, X. F.; Sultana, C. M.; Trueblood, J.; Hill, T. C. J.; Malfatti, F.; Lee, C.;  
771 Laskina, O.; Moore, K. A.; Beall, C. M.; McCluskey, C. S.; Cornwell, G. C.; Zhou, Y. Y.;  
772 Cox, J. L.; Pendergraft, M. A.; Santander, M. V.; Bertram, T. H.; Cappa, C. D.; Azam,  
773 F.; DeMott, P. J.; Grassian, V. H.; Prather, K. A. Microbial Control of Sea Spray  
774 Aerosol Composition: A Tale of Two Blooms. *Acs Central Science* **2015**, *1* (3),  
775 124-131.  
776 66. Compiano, A. M.; Romano, J. C.; Garabetian, F.; Laborde, P.; Delagiraudiere,  
777 I. Monosaccharide composition of particulate hydrolyzable sugar fraction in  
778 surface microlayers from brackish and marine waters. *Mar. Chem.* **1993**, *42* (3-  
779 4), 237-251.  
780 67. Aller, J. Y.; Kuznetsova, M. R.; Jahns, C. J.; Kemp, P. F. The sea surface  
781 microlayer as a source of viral and bacterial enrichment in marine aerosols.  
782 *Journal of Aerosol Science* **2005**, *36* (5-6), 801-812.  
783 68. Miralto, A.; Barone, G.; Romano, G.; Poulet, S. A.; Ianora, A.; Russo, G. L.;  
784 Buttino, I.; Mazzarella, G.; Laabir, M.; Cabrini, M.; Giacobbe, M. G. The insidious  
785 effect of diatoms on copepod reproduction. *Nature* **1999**, *402* (6758), 173-176.  
786 69. Stonik, V.; Stonik, I. Low-Molecular-Weight Metabolites from Diatoms:  
787 Structures, Biological Roles and Biosynthesis. *Marine Drugs* **2015**, *13* (6), 3672.  
788 70. Prestegard, S.; Erga, S.; Steinrücken, P.; Mjøs, S.; Knutsen, G.; Rohloff, J.  
789 Specific Metabolites in a *Phaeodactylum tricornutum* Strain Isolated from  
790 Western Norwegian Fjord Water. *Marine Drugs* **2016**, *14* (1), 9.  
791 71. Wichard, T.; Pohnert, G. Formation of halogenated medium chain  
792 hydrocarbons by a lipoxygenase/hydroperoxide halolyase-mediated  
793 transformation in planktonic microalgae. *Journal of the American Chemical*  
794 *Society* **2006**, *128* (22), 7114-7115.  
795 72. Pohnert, G. Wound-activated chemical defense in unicellular planktonic  
796 algae. *Angewandte Chemie-International Edition* **2000**, *39* (23), 4352-+.  
797 73. Wolfe, G. V.; Steinke, M.; Kirst, G. O. Grazing-activated chemical defence in  
798 a unicellular marine alga. *Nature* **1997**, *387* (6636), 894-897.  
799 74. Cochran, R. E.; Laskina, O.; Jayarathne, T.; Laskin, A.; Laskin, J.; Lin, P.;  
800 Sultana, C.; Lee, C.; Moore, K. A.; Cappa, C. D.; Bertram, T. H.; Prather, K. A.;  
801 Grassian, V. H.; Stone, E. A. Analysis of Organic Anionic Surfactants in Fine and  
802 Coarse Fractions of Freshly Emitted Sea Spray Aerosol. *Environ. Sci. Technol.*  
803 **2016**, *50* (5), 2477-2486.  
804 75. Bruggemann, M.; Hayeck, N.; Bonnineau, C.; Pesce, S.; Alpert, P. A.; Perrier,  
805 S.; Zuth, C.; Hoffmann, T.; Chen, J.; George, C. Interfacial photochemistry of  
806 biogenic surfactants: a major source of abiotic volatile organic compounds.  
807 *Faraday Discussions* **2017**, *200*, 59-74.  
808 76. Zhou, S.; Gonzalez, L.; Leithead, A.; Finewax, Z.; Thalman, R.; Vlasenko, A.;  
809 Vagle, S.; Miller, L. A.; Li, S. M.; Bureekul, S.; Furutani, H.; Uematsu, M.; Volkamer,  
810 R.; Abbatt, J. Formation of gas-phase carbonyls from heterogeneous oxidation of  
811 polyunsaturated fatty acids at the air-water interface and of the sea surface  
812 microlayer. *Atmos. Chem. Phys.* **2014**, *14* (3), 1371-1384.  
813 77. Hung, H. M.; Ariya, P. Oxidation of oleic acid and oleic acid/sodium  
814 chloride(aq) mixture droplets with ozone: Changes of hygroscopicity and role of  
815 secondary reactions. *J. Phys. Chem. A* **2007**, *111* (4), 620-632.

816 78. Kind, T.; Fiehn, O. Metabolomic database annotations via query of  
817 elemental compositions: Mass accuracy is insufficient even at less than 1 ppm.  
818 *Bmc Bioinformatics* **2006**, *7*, 10.  
819 79. Tolić, N.; Liu, Y.; Liyu, A.; Shen, Y.; Tfaily, M. M.; Kujawinski, E. B.;  
820 Longnecker, K.; Kuo, L.-J.; Robinson, E. W.; Paša-Tolić, L.; Hess, N. J. Formularity:  
821 Software for Automated Formula Assignment of Natural and Other Organic  
822 Matter from Ultrahigh-Resolution Mass Spectra. *Anal. Chem.* **2017**, *89* (23),  
823 12659-12665.  
824  
825